catalysts

MDPI

Article

The Effect of Potassium Inclusion in a Silver Catalyst for N_2O-Mediated Oxidation of Soot in Oxidising Exhaust Gases

Anna Cooper, Stan Golunski and Stuart H. Taylor *

Cardiff Catalysis Institute, School of Chemistry, Cardiff University, Main Building, Park Place, Cardiff CF10 3AT, UK; anniecooper10@btinternet.com (A.C.); segolunski@gmail.com (S.G.)
* Correspondence: taylorsh@cardiff.ac.uk

Abstract: It has previously been shown that an Ag/CZA catalyst can simultaneously remove NOx and soot from an oxygen-rich exhaust gas at low temperatures, by utilising the N_2O generated preferentially during incomplete NOx reduction. Here, we examine the effect of reformulating the catalyst to include potassium, which is a known promoter of soot combustion. On including 2 wt% K, NOx-reduction occurs both in the absence and presence of soot, but the N_2O formed does not play a part in the oxidation of soot. At higher K loadings (5, 10 and 15 wt%), NOx reduction is almost completely disabled, and only contributes to the activity of the catalyst containing 5 wt% K when tested in the presence of soot. At a loading of 20 wt% K, the potassium phase segregates, leaving NO and NH_3 adsorption sites exposed. In the absence of soot, this catalyst can remove NOx by reduction on the Ag/CZA component and through nitration of the potassium phase. Although the presence of potassium lowers the onset temperature for soot oxidation to within the range of NOx reduction over Ag/CZA, the mobile K species prevents the desirable C+N_2O reaction.

Keywords: soot oxidation; NOx reduction; silver; ceria-zirconia; environmental catalysts

Citation: Cooper, A.; Golunski, S.; Taylor, S.H. The Effect of Potassium Inclusion in a Silver Catalyst for N_2O-Mediated Oxidation of Soot in Oxidising Exhaust Gases. *Catalysts* **2022**, *12*, 753. https://doi.org/10.3390/catal12070753

Academic Editors: Yu Huang and Qian Zhang

Received: 26 May 2022
Accepted: 5 July 2022
Published: 7 July 2022

1. Introduction

Many countries have set ambitious targets for the transition to electrically powered vehicles [1]. For example, the target is 30% of all new vehicles by 2030 in India [2], 50% by 2030 in the USA, and 100% by 2035 in the EU [3]. Even so, it will be 2–3 decades before the global transportation fleet is no longer reliant on the internal combustion engine, and perhaps even longer if e-fuels (hydrocarbons manufactured by reaction of waste CO_2 with *green hydrogen*) are proven to have an advantage over batteries in terms of lifecycle CO_2 emissions [3]. In the meantime, there will still be a need for improved aftertreatment technologies as ever more demanding emissions legislation comes into force, such as the Euro 7 standards [4] which are expected to take effect from 2025.

The exhaust gas released by a gasoline (petrol) internal combustion engine can be treated very effectively using a three-way catalytic converter, which is a single aftertreatment unit designed to operate over a broad range of temperatures in an exhaust gas close to the stoichiometric air/fuel ratio [5]. By contrast, a diesel engine requires a more complex aftertreatment system, mainly because the exhaust gas is cooler and it contains (i) soot particulate (which requires trapping before it can be oxidised) and (ii) a high concentration of O_2 (which makes the reduction of NOx particularly challenging) [6]. Most commercial systems currently consist of a series of consecutive units [7,8], e.g., a diesel oxidation catalyst (DOC) for the removal of carbon monoxide and hydrocarbons, a diesel particulate filter (DPF) for trapping soot, and an SCR catalyst for the selective reduction of NOx by reaction with ammonia which is formed in situ by dosing aqueous urea into the exhaust gas. The DOC has the additional function of intermittently generating a large exotherm to induce combustion of the trapped soot, which regenerates the DPF. This is achieved by injecting some of the diesel fuel upstream of the DOC, though at the cost of lowering the fuel economy and increasing the CO_2 emissions of the vehicle.

Although an SCR catalyst can be coated onto a DPF to form an integrated unit (referred to as SCRF [7], SCRoF [8] or SPDF [9]), the filter still requires active regeneration by the injection of fuel into an upstream DOC. Therefore, the challenge remains to design a catalysed filter in which the chemistry of NOx-reduction is coupled with that of continuous soot oxidation [10] (e.g., using perovskites [11] or 3DOM mixed-metal oxides [12]), so avoiding the requirement for intermittent regeneration of the filter. We have previously shown [13,14] that catalysts based on Ag/CZA (silver supported on ceria–zirconia–alumina), in which the functions of incomplete NOx reduction and soot oxidation are combined, have the potential to control soot particulate and NOx emissions at the low temperatures typical of the exhaust gas emitted by the engine of a diesel passenger car. These catalysts can oxidise immobilised soot through several different pathways. At low exhaust-gas temperatures, the oxidising species is the product of incomplete NOx reduction (i.e., N_2O or its precursor on the catalyst surface), before NO_2 and then O_2 take over at higher temperatures.

In this study, we have examined the effect of potassium addition on the performance of Ag/CZA for the simultaneous removal of NOx and soot. Although alkali metal can block the acid sites needed for NH_3 and NO adsorption [15], it is an active carbon combustion catalyst in its own right [16] and a known promoter of Ag/CZA for diesel soot combustion [17]. It can also interfere with the redox cycle in metal oxide SCR catalysts [18], suggesting that its inclusion could increase N_2O production by promoting incomplete NOx reduction. This work represents the first stage in the optimisation of the Ag-K/CZA catalyst system, in which the ultimate objectives are to improve the NOx-reduction activity while further lowering the onset temperature for soot oxidation, without allowing the escape of any unconverted N_2O.

2. Results and Discussion

Figures 1 and 2 show the key results from a previous study [13], which had led us to conclude that the simultaneous control of NOx and soot can be achieved at low exhaust-gas temperatures by coupling two reactions that do not feature in conventional SCR, DOC and DPF units. This alternative approach relies on using a NOx-reduction catalyst (Ag/CZA), which generates N_2O between 220 and 410 °C (Figure 1). When this catalyst is loosely mixed with carbon black (a diesel soot mimic), no N_2O is detected during testing under the same conditions (Figure 2). The oxidation of soot takes place in a series of four steps, with the temperature range of the first step coinciding with the position of the N_2O peak when the catalyst alone is tested. By analysing the gas composition exiting the microreactor when the catalyst was tested in the absence/presence of carbon black [13], we were able to resolve these four steps in the destruction of soot over Ag/CZA:

(i) Catalysed oxidation by N_2O to form CO_2 and N_2;
(ii) Non-catalysed oxidation by NO_2 to form CO_2 and re-form NO;
(iii) Catalysed oxidation by O_2 to form CO_2;
(iv) Non-catalysed oxidation by O_2 to form CO and CO_2.

In aiming to optimise the soot and NOx performance of Ag/CZA as a function of temperature, our rationale for adding potassium was to lower the onset temperature for $C+O_2$, so as to avoid the step in which NO is re-formed through the non-catalysed $C+NO_2$ reaction. This would mean that the removal of soot under light-duty diesel conditions would occur only through oxidation by N_2O and O_2. Our earlier studies had shown that a relatively high loading of potassium ($\geq$10 wt%) needs to be added to Ag/CZA in order to lower the onset temperature for catalytic combustion of the elemental carbon in diesel soot to within the typical temperature range for the exhaust emitted by diesel passenger cars [19]. Therefore, in this study, we have started from a high loading of 20 wt% K in Ag/CZA, before testing catalysts with the lower loadings of 15, 10, 5 and 2 wt%.

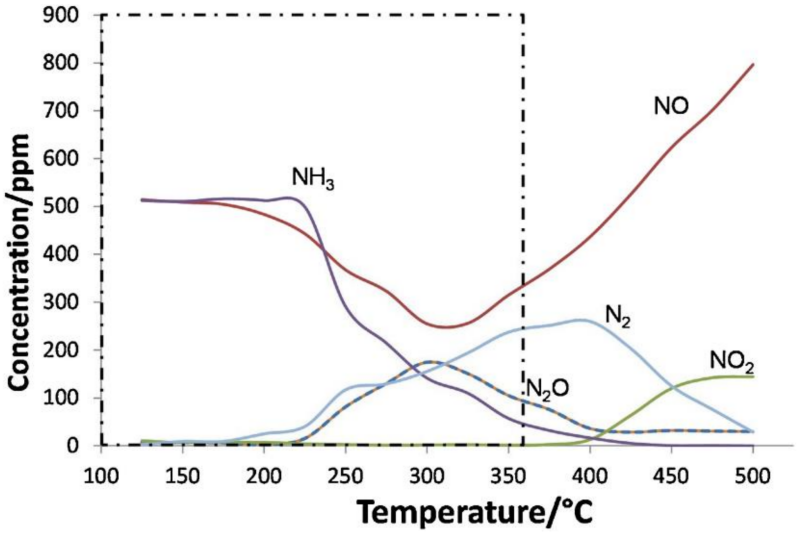

Figure 1. NOx reduction over K-free Ag/CZA using NH_3 as reductant. Dotted line indicates typical 'temperature window' for diesel exhaust emitted by passenger cars. This figure was published in *Applied Catalysis B*, 239, Davies et al., Simultaneous removal of NOx and soot particulate from diesel exhaust by in-situ catalytic generation and utilisation of N_2O [13]. 2018, Elsevier.

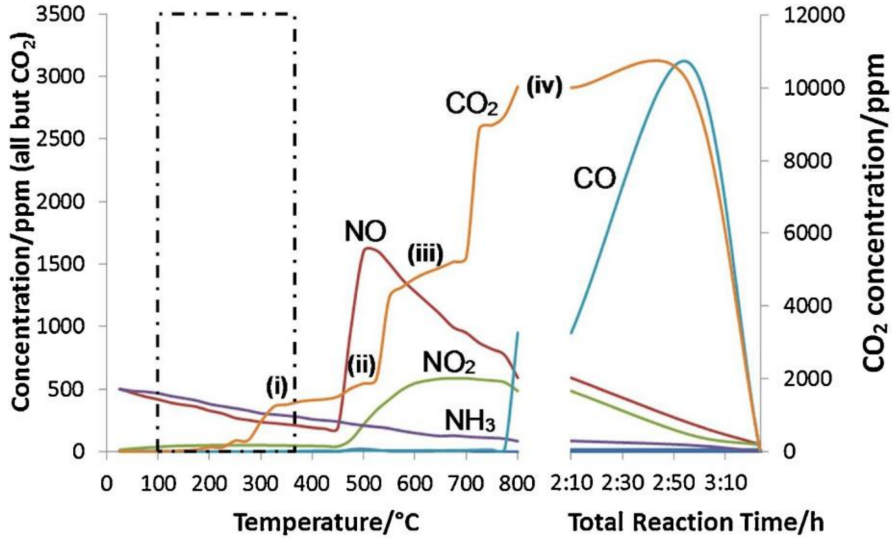

Figure 2. NOx reduction and soot oxidation when K-free Ag/CZA is mixed with carbon black. Dotted line indicates typical 'temperature window' for diesel exhaust emitted by passenger cars. The four consecutive steps for carbon oxidation are indicated (i)–(iv). This figure was published in *Applied Catalysis B*, 239, Davies et al., Simultaneous removal of NOx and soot particulate from diesel exhaust by in-situ catalytic generation and utilisation of N_2O [13]. 2018, Elsevier.

When 2%Ag–20%K/CZA was tested for the reduction of NOx by NH_3 in the absence of carbon black (Figure 3a), there was a decrease in NO concentration between 175 and 250 °C, which was accompanied by an equivalent decrease in NH_3 concentration, and coincided with the appearance of N_2O. This behaviour is consistent with incomplete NOx reduction, which leads to a product-selectivity of approximately 1:1 of N_2O and N_2. However, the reaction was almost completely suppressed as the temperature approached 300 °C, while at the same time there was rapid evolution of CO_2 which gave rise to a distinct peak centred at 325 °C.

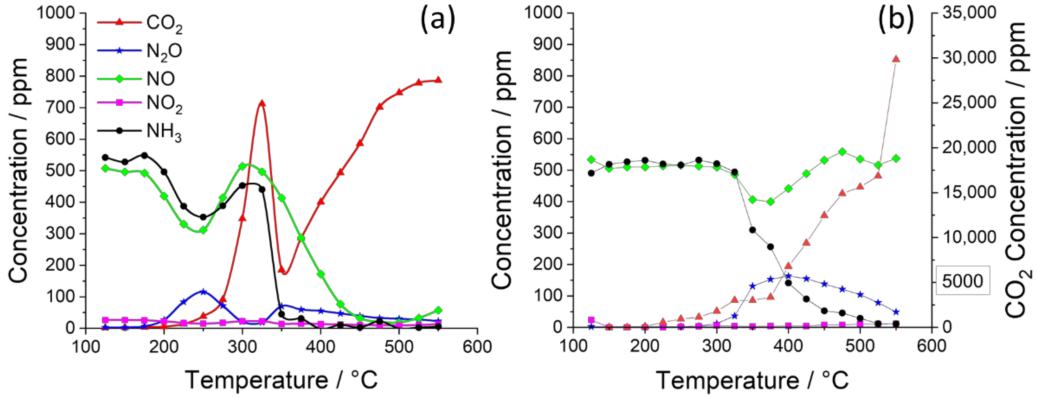

Figure 3. Performance of 2%Ag–20%K/CZA tested in a simulated exhaust gas containing NH_3 as reductant (**a**) in the absence of carbon black, and (**b**) in the presence of carbon black. This figure contains data from a previous publication [14]. 2020, MDPI.

There was also a more gradual evolution of CO_2 at lower temperatures, which was observed for all catalysts in the absence of carbon black (see later figures) and which can be attributed to the decomposition of residual CZA-carbonates (which are known to persist even after calcination [20]) and the dissociation of carbonate and hydrogencarbonate species on the CZA surface (having formed by adsorption of CO_2 and H_2O from ambient atmosphere during storage and handling of the catalyst sample). However, the distinct CO_2 peak observed was specific to this catalyst. A previous *operando* study of a K_2CO_3/Al_2O_3 catalyst during soot combustion, showed that the potassium was initially present as a mixture of hydrated K_2CO_3 and $KHCO_3$, before transforming into well-defined K_2CO_3 [21]. As the transformation from $KHCO_3$ to K_2CO_3 releases CO_2 (and H_2O), it seems likely that this is the cause of the CO_2 peak for 2%Ag–20%K/CZA (see also Supplementary Materials). The steep rise in CO_2 concentration that follows the peak (and reaches a plateau at 550 °C) mirrors the decline in NO concentration, which is consistent with the potassium transforming from K_2CO_3 to KNO_3 at higher temperatures. Carbonate to nitrate transformation is a key mechanism by which alkali metals and alkaline earth metals function as NOx storage materials in exhaust-gas streams [22].

Unlike the K-free Ag/CZA catalyst (Figure 1), which shows an inversion in the NO trace at about 320 °C, as the direct oxidation of NH_3 to NO (and NO_2) becomes the dominant reaction, the 2%Ag–20%K/CZA catalyst shows a continuous decline in NO concentration between 300 and 450 °C (Figure 3a). The performance over the high temperature range is consistent with 2%Ag–20%K/CZA now functioning primarily as an NH_3-oxidation catalyst and a NOx storage material, so that the gas phase NO and the NOx formed by NH_3 oxidation are stored as nitrate species, explaining why the gas phase concentrations of NH_3, NO and NO_2 all decline to zero.

The CO_2-evolution peak at 325 °C seems particularly significant, marking the transition in 2%Ag–20%K/CZA from NOx reduction to NOx storage. However, XRD did not reveal any definite changes in the bulk crystal structure of the catalyst at this temperature. The initial and final full-range scans (before and after the catalyst was heated to 600 °C under flowing air) show diffraction peaks typical of CeO_2 (28°, 33°, 47°, 56°) [23] and Ag (37.2°, 43.4°), while K_2CO_3 appears as a discrete peak centred at 32.0° and as a shoulder (37.3°) on the Ag peak at 37.2° (Figure 4).

Several small and reversible changes were observed in the diffraction pattern during temperature-programmed XRD (Figure 5): two Al_2O_3 peaks at 39.7° and 40.8° [24] were clearly visible at 100 °C, but their intensity decreased during heating, before they merged at 550 °C; the peaks associated with Ag and K_2CO_3 shifted slightly in position. These changes can be attributed to thermally induced expansion of the lattice parameters of the component phases of the catalyst [25,26]. The absence of any substantial change in the bulk

of the catalyst, therefore, suggests that the transition from $KHCO_3$ to K_2CO_3 at 325 °C is primarily a surface effect.

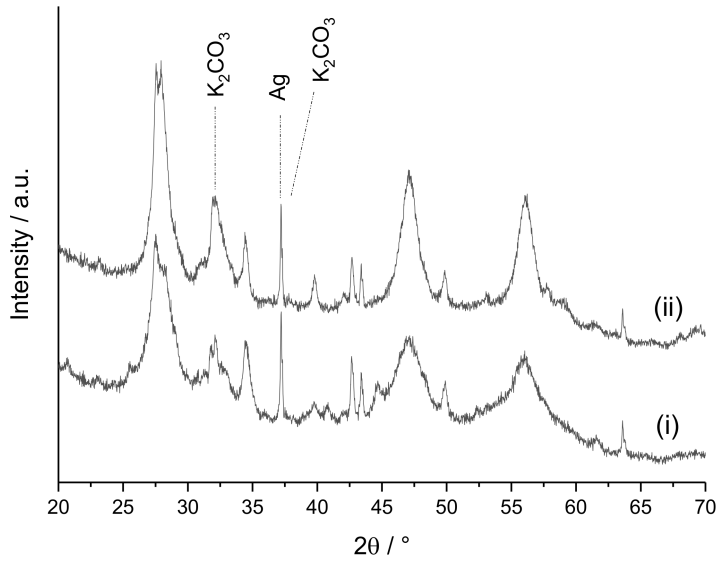

Figure 4. Full-range scan diffraction pattern for 2%Ag–20%K/CZA (i) before and (ii) after temperature-programmed XRD analysis.

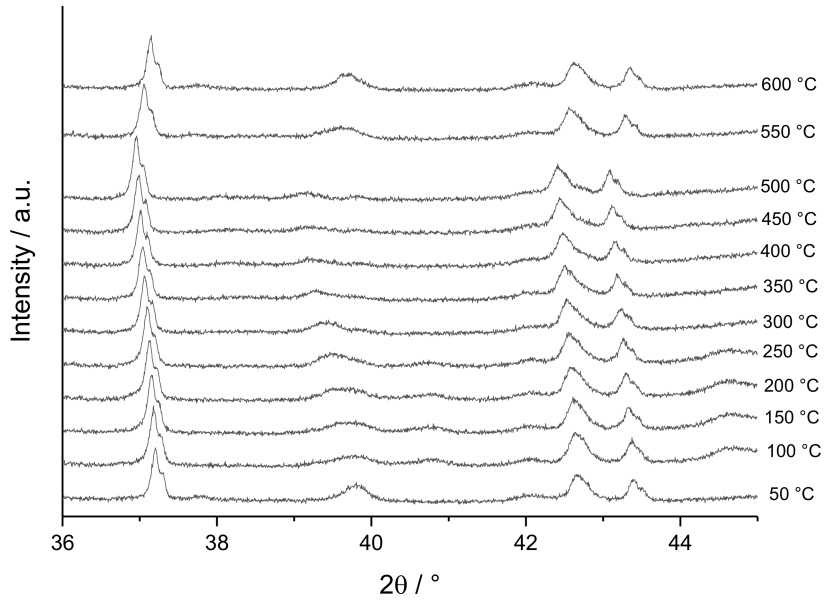

Figure 5. Temperature-programmed XRD analysis of 2%Ag–20%K/CZA.

In the presence of carbon black (Figure 3b), 2%Ag–20%K/CZA showed little activity at temperatures below 300 °C, except for the gradual release of CO_2 from the dissociation of carbonate and hydrogencarbonate species on the CZA surface. Compared with the catalyst alone (Figure 3a), the onset of NOx reduction and the associated formation of N_2O were delayed by about 100 °C. Although K_2CO_3 has a Tammann temperature of 309 °C, it can become mobile at temperatures as low as 200 °C when it is in the presence of soot [21]. This form of *reaction-induced spreading* [27] could explain the suppression of NOx reduction below 300 °C and the inhibition of the C+N_2O reaction, but it also has the beneficial effect of promoting oxidation of carbon black by reaction with other oxidants. The onset of carbon oxidation (at about 300 °C) correlates closely with the transition from NOx reduction to ammonia oxidation and NOx storage, which occurred when the catalyst alone was tested.

These results suggest, therefore, that initially carbon reacts with stored nitrate species (to form CO_2 and re-form NO) before the C+O_2 reaction predominates. The activity of this catalyst for soot destruction, as measured by the rate of CO_2 formation, is about three times that of K-free 2%Ag/CZA at 300 °C and about 7.5 times at 500 °C, but it only converts a maximum of 20% of the inlet NO.

At loadings of 15 and 10 wt% potassium, the performance curves are much simpler (Figures 6 and 7). In the absence of carbon black (Figure 6a), 2%Ag–15%K/CZA showed very little change in NO concentration over the entire temperature range, suggesting that the NO-adsorption sites (on the Ag) were blocked by potassium; while the concentration of NH_3 only began to decrease above 300 °C, suggesting that NH_3-adsorption sites (on the CZA) were exposed when the K_2CO_3 became mobile as it reached its Tammann temperature. The decline in NH_3 concentration coincided with a higher rate of CO_2 evolution. Once again, this is consistent with NH_3 being oxidised to NOx, which is stored by the potassium through the transformation of K_2CO_3 to KNO_3 and the release of CO_2. Very similar behaviour was observed for 2%Ag–10%K/CZA (Figure 7a), except that more NO was released towards the end of the test, reflecting the lower NOx storage capacity arising from the lower loading of potassium in this catalyst.

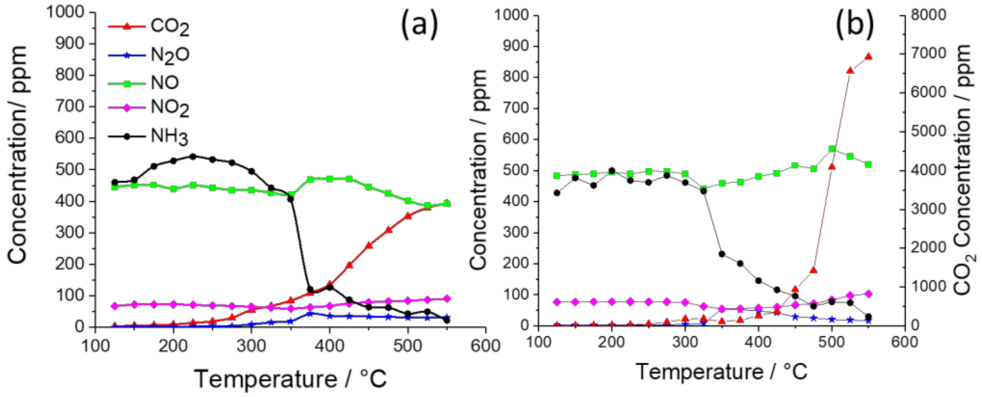

Figure 6. Performance of 2%Ag–15%K/CZA tested in a simulated exhaust gas containing NH_3 as reductant (**a**) in the absence of carbon black, and (**b**) in the presence of carbon black.

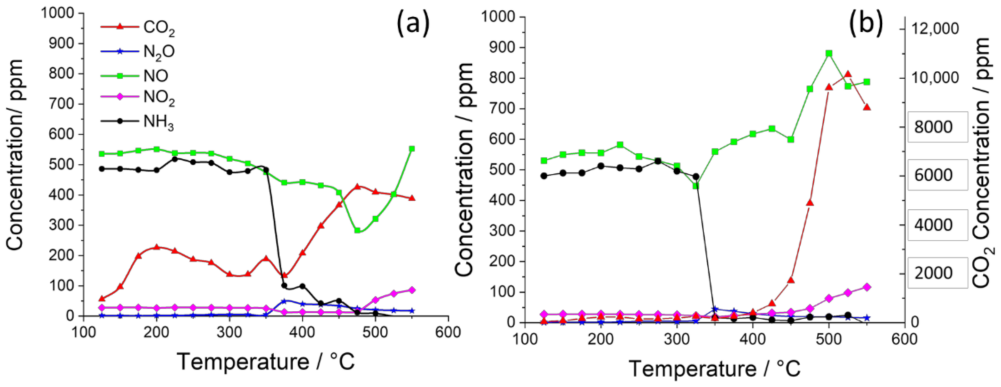

Figure 7. Performance of 2%Ag–10%K/CZA tested in a simulated exhaust gas containing NH_3 as reductant (**a**) in the absence of carbon black, and (**b**) in the presence of carbon black.

XPS analysis of 2%Ag–10%K/CZA, before and after testing in the absence of carbon black (Table 1), showed a reduction in surface concentrations of Ag, K, Al and carbonate, while the concentrations of Ce and Zr increased. These changes can be explained by the mobility of K_2CO_3 and its transformation to KNO_3. When the K_2CO_3 becomes mobile it can cover more of the Ag surface where the NO adsorption sites are located, but it can also migrate deep into the pore structure of the CZA, so exposing more of the external

surface which provides NH_3 adsorption sites. The decrease in surface carbonate concentration can be accounted for in part by the subsurface migration of K_2CO_3, but also by its nitration. Significantly, the post-reaction spectrum revealed that the K2p peaks had shifted to higher binding energies (Figure 8), which is consistent with a change in the local chemical environment brought about by nitration of the potassium. It is also worth noting that the transformation from K_2CO_3 to KNO_3 would result in even greater mobility of the potassium, because KNO_3 has a much lower Tammann temperature (30.5 °C) than K_2CO_3 (309 °C).

Table 1. Surface composition of 2%Ag–10%K/CZA before and after testing in absence of soot, as determined by XPS.

	Ag	C (Carbonate)	K	Ce	Al	O	Zr
Before testing	1.0	5.6	18.6	12.9	16.5	37.6	3.3
After testing	0.6	3.7	12.3	24.1	13.0	32.1	5.6

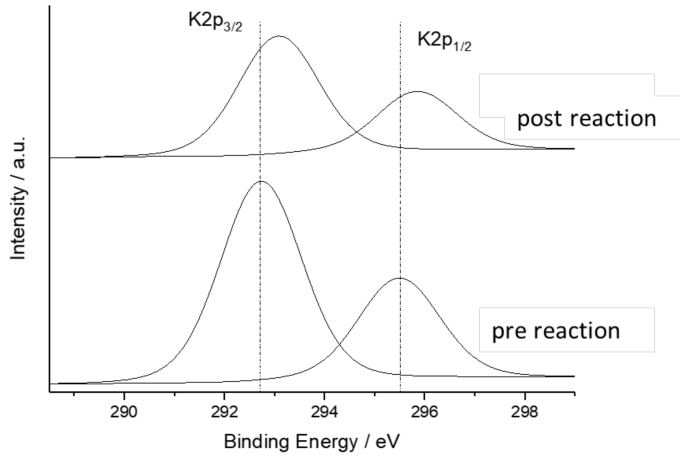

Figure 8. K2p bands in XPS spectrum of 2%Ag–10%K/CZA before testing (pre-reaction) and after testing (post-reaction) in the absence of carbon black.

When tested in the presence of carbon black, neither 2%Ag–15%K/CZA (Figure 6b) nor 2%Ag–10%K/CZA (Figure 7b) showed any marked differences in NO or NH_3 activity below 450 °C compared with the tests in the absence of carbon black (Figures 6a and 7a). For both catalysts, rapid formation of CO_2 began at about 375 °C. As this is above the onset temperature for the Ag-K/CZA-catalysed combustion of diesel soot under a synthetic exhaust gas without added NH_3 [17], it seems safe to conclude that the C+O_2 reaction is the predominant source of CO_2 over 2%Ag–15%K/CZA and 2%Ag–10%K/CZA. Only at temperatures above 450 °C was there any sign of nitrogenous species being involved in the oxidation of the carbon. This is seen more clearly in the case of 2%Ag–10%K/CZA (Figure 7b), where there is a peak in NO concentration (and a coincident peak in CO_2) at high temperature, suggesting that the carbon was reacting with stored nitrate species to form CO_2 and re-form NO.

Although the NOx performance of 2%Ag–5%K/CZA (Figure 9a) was quite similar to that of 2%Ag–10%K/CZA (Figure 7a) in the absence of carbon black, there were significant differences between these catalysts when carbon black was present (compare Figure 7b with Figure 9 b). In fact, the performance of 2%Ag–5%K/CZA in the presence of soot (Figure 9b) showed several of the features of K-free Ag/CZA (Figure 1): namely, incomplete NOx reduction (with N_2O formation) below 450 °C, followed by NH_3 oxidation to NO and NO_2 at higher temperatures. These results imply that, in the presence of carbon black, potassium mobility can expose more of the Ag surface (allowing NO adsorption

and hence its reduction to take place), but it also has the detrimental effect of blocking the C+N_2O reaction by which low-temperature soot oxidation can take place. Therefore, in common with 2%Ag–10%K/CZA and 2%Ag–15%K/CZA, the oxidation of carbon takes place primarily by the C+O_2 reaction, with its signature onset-temperature of 375 °C.

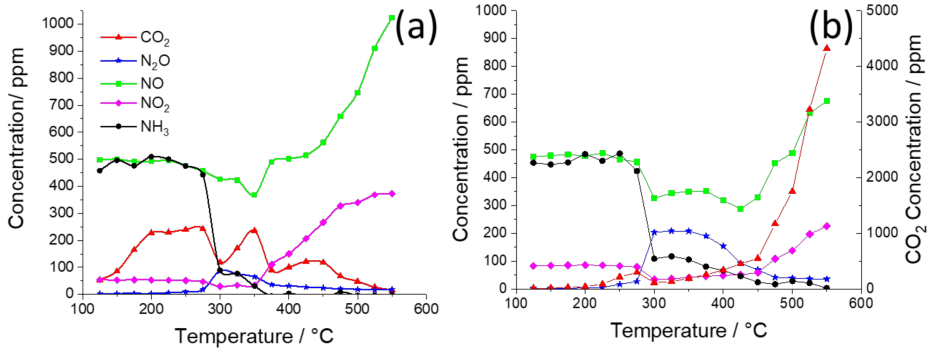

Figure 9. Performance of 2%Ag–5%K/CZA tested in a simulated exhaust gas containing NH_3 as reductant (**a**) in the absence of carbon black, and (**b**) in the presence of carbon black.

Both in the absence and presence of carbon black, 2%Ag–2%K/CZA (Figure 10) functioned as a NOx-reduction catalyst below 300 °C, before NH_3 oxidation predominated at higher temperatures. The onset temperature for NO and NH_3 conversion (200 °C) closely matched that of K-free Ag/CZA, as did the amount of NO converted, indicating that the potassium was having a negligible effect on the active sites located on the Ag and the CZA. From BET data (see Supplementary Materials), it was calculated that 6.02×10^{-8} mol g^{-1} of K ions would be required for monolayer coverage of the CZA support, which is much less than the theoretical concentration (4.99×10^{-4} mol g^{-1}) of K in 2%Ag–2%K/CZA. Therefore, the catalytic performance suggests that much of the K_2CO_3 was incorporated into the catalyst bulk and/or was present as discrete crystallites on the catalyst surface. There were some small but clear changes within the NOx-reduction regime when carbon black was present (Figure 10b), such that the NO and NH_3 conversions were lower, while the N_2O formation peak became larger. These changes are consistent with reaction-induced spreading of potassium (i) blocking NO and NH_3 adsorption sites, (ii) increasing the N_2O selectivity during NOx reduction, and (iii) inhibiting the C+N_2O reaction.

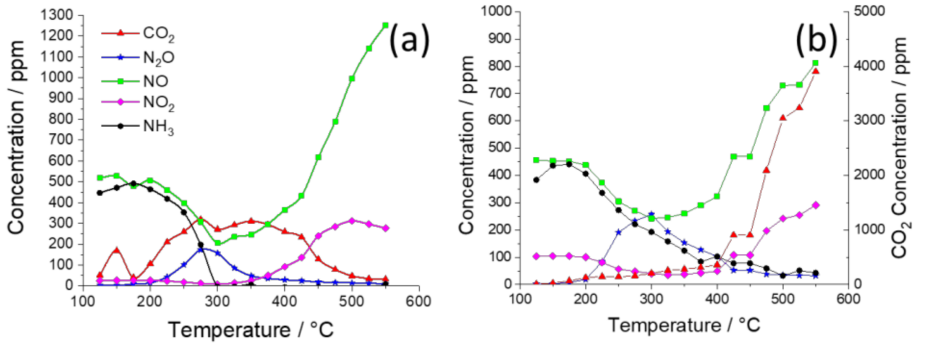

Figure 10. Performance of 2%Ag–2%K/CZA tested in a simulated exhaust gas containing NH_3 as reductant (**a**) in the absence of carbon black, and (**b**) in the presence of carbon black.

Again, in common with the catalysts containing 5, 10 and 15 wt% K, the dominant route to CO_2 over 2%Ag–2%K/CZA was via the C+O_2 reaction, with an onset temperature of 375 °C. This was 150 °C lower than the onset temperature for the C+O_2 reaction over K-free Ag/CZA, but it still lies just outside the upper limit of the typical temperature window for diesel exhaust emitted by the engine of a passenger car (see Figures 1 and 2).

3. Materials and Methods

3.1. Catalyst Preparation

The parent catalyst was 2 wt% Ag supported on co-precipitated ceria–zirconia–alumina (CZA) with an atomic composition of $Ce_{0\cdot35}Zr_{0.15}Al_{0.5}O_{1.75}$ (or 47 wt% Ce, 13 wt% Zr, and 40 wt% O). This catalyst had previously been shown to be active for N_2O-mediated soot oxidation [13]. A precipitating agent, aqueous sodium carbonate (1 M), was added to a precursor solution containing appropriate volumes of ammonium cerium (IV) nitrate (0.25 M), zirconium (IV) oxynitrate (0.25 M), and aluminium nitrate nonahydrate (0.25 M), at a pH of 9 and a temperature of 80 °C. The suspension that formed was aged for 1 h, before the precipitate was collected by filtration under vacuum, washed (2 L hot de-ionised water), dried (110 °C, 16 h) and calcined at 500 °C for 5 h in flowing air. The CZA support was then impregnated with aqueous solutions containing $AgNO_3$ (99.9999%, Sigma Aldrich, Gillingham, U.K.) and varying amounts of K_2CO_3 (99.9%, Fisher Scientific, Loughborough, U.K.) followed by drying (110 °C, 16 h) and calcination (flowing air, 500 °C, 5 h) to produce catalysts with the required weight loadings: 2%Ag–2%K/CZA, 2%Ag–5%K/CZA, 2%Ag–10%K/CZA, 2%Ag–15%K/CZA, 2%Ag–20%K/CZA.

3.2. Catalyst Performance Testing

Catalysts were tested in a fixed bed microreactor, using an online Gasmet FTIR process gas analyser (Gasmet Technologies U.K. Ltd., Northampton, UK) to measure the inlet and outlet gas concentrations. A simulated diesel exhaust gas comprising 500 ppm NO, 500 ppm NH_3, 8% O_2, and balance N_2 (total flow rate = 200 cm^3 min^{-1}, GHSV = 40,000 h^{-1}) was fed through a bed of either 0.25 g catalyst or 0.25 g of catalyst and 0.025 g of carbon black. Although CO_2 and H_2O are both present at concentrations of about 12% in diesel exhaust gas, at such high levels it would be difficult to detect relatively small changes in their concentrations. We, therefore, excluded CO_2 and H_2O from our simulated exhaust gas, so that their formation could be detected and used to track changes associated with the catalysts.

The mixed bed of catalyst and carbon black was prepared by shaking the two components together (in a 10:1 wt ratio), which was intended to represent the loose contact formed between a catalytic washcoat and soot in a catalysed soot filter [28]. The microreactor was heated (in a horizontal tube furnace) from 125 to 550 °C at a rate of 7 °C min^{-1}, with concentration measurements being recorded after the gas analysis had stabilised after every 25 °C increment. Using this test protocol, we were trying to mimic the conditions in a catalysed filter after start-up of the engine, when soot initially accumulates on the cold filter before the temperature is high enough for the catalyst to become active.

In presenting our test results, we plot the concentrations of reactant and product gases (in mol ppm) as a function of temperature, which is contrary to the convention in emission control catalysis where it is usual to show how the *conversion* of reactant gases changes with temperature (e.g., see [29]). Our figures draw attention to the formation of N_2O and CO_2, which are key measures of NOx-reduction and soot-oxidation functionality in the Ag/CZA and Ag-K/CZA catalysts.

3.3. Temperature-Programmed XRD

X-ray diffraction (XRD) was carried out on powder samples using a PANalytical X'pert Pro diffractometer (Malvern Panalytical Ltd., Malvern, U.K.) with a Cu X-ray source operating at 40 keV and 40 mA, with Kα1 X-rays selected using a Ge (111) single crystal monochromator. The diffractometer was fitted with an Anton-Parr in-situ cell, with an internal volume of 500 cm^3, which was used to monitor phase changes while a catalyst sample was heated under flowing air (20 cm^3 min^{-1}). After an initial full-scan was taken at ambient temperature, the sample was heated to 50 °C and held for 10 min before 2 diffraction patterns were collected over the range 36–44°. The temperature was then increased at a rate of 10 °C min^{-1}, in 50 °C increments, to a maximum of 600 °C; after each

increment, the temperature was held for 10 min before 2 scans (36–44°) were taken. A final full-scan was taken after the sample had been cooled to ambient temperature.

3.4. XPS

Surface analysis by X-ray photoelectron spectroscopy (XPS) was carried out on the catalysts using a Kratos Axis Ultra DLD photoelectron spectrometer (Kratos Analytical Ltd., Manchester, U.K.), with monochromatic AlKα radiation operating at an energy of 120 W (10 × 12 kV). The data were analysed using CasaXPS and modified Wagner sensitivity factors, as supplied by the instrument manufacturer, after subtraction of a Shirley background. All spectra were calibrated to the adventitious C (1s) line at 284.8 eV. The amount of surface carbonate was calculated using the C (1s) signals associated with C–O–C and C–O=C.

4. Conclusions

N_2O-mediated soot oxidation is distinct from other methods being evaluated for the simultaneous removal of NOx and soot from fuel-lean exhaust gases. Its main advantage is that the soot+N_2O reaction occurs at lower temperatures than established soot oxidation reactions. However, in coupling incomplete NOx reduction with soot oxidation, one of the major risks is that there will be an imbalance between the rates of N_2O formation and soot oxidation, resulting in the undesirable release of N_2O, which has a high global-warming potential [30]. In this study, we have examined the effect of alkali metal (known to catalyse combustion) on both soot oxidation and NOx reduction over Ag/CZA, which has previously been shown to be an active and durable catalyst for these reactions, including when coated onto a filter and tested under real exhaust gas [13].

We have found that inclusion of potassium, as K_2CO_3, in a 2%Ag/CZA catalyst has the expected effect of promoting its soot oxidation activity. However, the potassium also induces pronounced changes in NOx adsorption and in its conversion by NH_3, which can vary depending on the potassium loading and on whether soot is present within the catalyst bed (as summarised in Table 2). In fact, our results show that the catalytic performance is very sensitive to changes in the surface concentration, location and composition of the potassium species, which means that catalyst testing has provided us with a form of reactive characterisation of the Ag-K/CZA system.

Table 2. Effects of potassium loading on NOx conversion and the onset of soot (carbon black) oxidation.

K Loading in 2%Ag–K/CZA	Maximum NOx Conversion (to N_2O and N_2)	Onset Temperatures of Steps in Soot Oxidation
0%	50% at 320 °C	220 °C: C+N_2O 450 °C: C+NO_2 525 °C: C+O_2
2%	45% at 300 °C	375 °C: C+O_2
5%	42% at 425 °C	375 °C: C+O_2
10%	19% at 350 °C	375 °C: C+O_2
15%	12% at 325 °C	375 °C: C+O_2
20%	20% at 375 °C	300 °C: C+nitrate 375 °C: C+O_2

Based on the key assumptions that Ag provides the NO adsorption sites and ceria-zirconia (in CZA) provides the NH_3 adsorption sites, we can draw the following conclusions from the performance data:

(i) Over the loading range of 5–15 wt% K, potassium blocks the majority of the NO-adsorption sites on the Ag and the low-temperature NH_3 adsorption sites on the CZA, when it forms multiple layers over the surface during catalyst preparation.

The NO-adsorption sites are partially restored on 2%Ag–5%K/CZA during testing in the presence of soot, when the potassium species become mobile and wet the soot particulate;

(ii) At both the lowest (2 wt%) and highest (20 wt%) K-loading, most of the NO adsorption sites and low-temperature NH_3 adsorption sites are available in the fresh catalysts, allowing NOx reduction to N_2O to take place. This suggests that, during preparation of 2%Ag–20%K/CZA, the K_2CO_3 segregates to leave exposed regions on the Ag and CZA surfaces;

(iii) Particularly at high K-loadings (15 and 20 wt%), the catalysts can function as NOx storage materials at temperatures > 300 °C, even when minimal NO adsorption is taking place. The likely pathway is by NH_3 adsorption on CZA, followed by oxidation to nitrate species, which displace the carbonate from the potassium as CO_2.

(iv) The main soot oxidation reaction over all these catalysts is C+O_2, which has an onset temperature of around 375 °C. The only other apparent soot oxidation route is by reaction with the nitrates formed during NOx storage; this reaction re-forms NO at the same time as forming CO_2;

(v) Potassium prevents N_2O-mediated oxidation of soot, which is the main mechanism by which soot destruction occurs over K-free Ag/CZA at the low temperatures typical of the exhaust emitted by light-duty diesel engines.

The mobility of the potassium is clearly a critical parameter in the activity of Ag-K/CZA catalysts, not just in terms of the oxidation of trapped soot, but also because the dynamic nature of the catalyst surface affects the activation of NOx and NH_3. Although the potassium is initially in the form of K_2CO_3, our results point to its transformation into KNO_3 under NOx reduction conditions. It is known that, when K_2CO_3 comes into contact with elemental carbon, it can undergo reduction to form K_2O [31]. However, in a previous *operando* study of K_2CO_3-catalysed carbon oxidation under simulated exhaust gas conditions [21], we did not detect the formation of K_2O. We therefore propose that the K_2CO_3 transforms directly to KNO_3 by interaction with adsorbed NO_2, which is formed primarily from the catalysed oxidation of the NH_3 that is added to the gas-stream as a NOx reductant.

Supplementary Materials: The following supporting information can be downloaded at: https://www.mdpi.com/article/10.3390/catal12070753/s1, CO_2 Trace Investigations—Figure S1: Evolution of CO_2 during heat treatment of 2%Ag–20%K/CZA at 300 °C; Figure S2: NOx reduction performance of 2%Ag–20%K/CZA (a) before and (b) after heat treatment at 300 °C; Figure S3: Evolution of CO_2 during heat treatment of 2%Ag–20%K/CZA at 500 °C; Figure S4: NOx reduction performance of 2%Ag–20%K/CZA (a) before and (b) after heat treatment at 500 °C; Temperature-programmed XRD—Figure S5: CZA; Figure S6: 2%Ag–2%K/CZA; Figure S7: 2%Ag–5%K/CZA; Figure S8: 2%Ag–10%K/CZA; Figure S9: 2%Ag–15%K/CZA.

Author Contributions: Conceptualization, S.G. and S.H.T.; data curation, A.C.; formal analysis, A.C.; resources, S.G.; supervision, S.G. and S.H.T.; writing—original draft, A.C., S.G. and S.H.T.; writing—review and editing, A.C. and S.H.T. All authors have read and agreed to the published version of the manuscript.

Funding: The authors gratefully acknowledge the support of the EPSRC Centre for Doctoral Training in Catalysis (funded by EPSRC: EP/L016443/1, Cardiff University and the Universities of Bath and Bristol).

Data Availability Statement: Primary data sets (used for the figures and tables) are available on request from the corresponding author.

Acknowledgments: We would like to express our thanks to James Hayward and David Morgan for running the XRD and XPS experiments, respectively.

Conflicts of Interest: The authors declare no conflict of interest.

References

1. Mali, B.; Shrestha, A.; Chapagain, A.; Bishwokarma, R.; Kumar, P.; Gonzalez-Longatt, F. Challenges in the penetration of electric vehicles in developing countries with a focus on Nepal. *Renew. Energy Focus* **2022**, *40*, 1–12. [CrossRef]
2. Chaturvedi, B.K.; Nautiyal, A.; Kandpal, T.C.; Yaqoot, M. Projected transition to electric vehicles in India and its impact on stakeholders. *Energy Sustain. Dev.* **2022**, *66*, 189–200. [CrossRef]
3. Garcia, A.; Monsalve-Serrano, J.; Villalta, D.; Tripathi, S. *Electric Vehicles vs e-Fuelled ICE Vehicles: Comparison of Potentials for Life Cycle CO_2 Emission Reduction*; SAE Technical Paper; SAE International: Warrendale, PA, USA, 2022.
4. Joshi, A. *Review of Vehicle Engine Efficiency and Emissions*; SAE Technical Paper; SAE International: Warrendale, PA, USA, 2022.
5. Twigg, M.V. Catalytic control of emissions from cars. *Catal. Today* **2011**, *163*, 33–41. [CrossRef]
6. Lambert, C.K. Current state of the art and future needs for automotive catalysis. *Nat. Catal.* **2019**, *21*, 554–557. [CrossRef]
7. Granger, P. Challenges and breakthroughs in post-combustion catalysis: How to match future stringent regulations. *Catal. Sci. Technol.* **2017**, *7*, 5195–5211. [CrossRef]
8. Martinovic, F.; Castoldi, L.; Deorsola, F.A. Aftertreatment technologies for diesel engines: An overview of the combined systems. *Catalysts* **2021**, *11*, 653. [CrossRef]
9. Purfürst, M.; Naumov, S.; Langeheinecke, K.-J.; Gläser, R. Influence of soot on ammonia adsorption and catalytic DeNOx-properties of diesel particulate filters coated with SCR-catalysts. *Chem. Eng. Sci.* **2017**, *168*, 423–436. [CrossRef]
10. Piumetti, M.; Bensaid, S.; Fino, D.; Russo, N. Catalysis in diesel engine NO*x* aftertreatment: A review. *Catal. Struct. React.* **2015**, *1*, 155–173.
11. Urán, L.; Gallego, J.; Ruiz, W.; Bailón-García, E.; Bueno-López, A.; Santamaría, A. Monitoring intermediate species formation by DRIFT during the simultaneous removal of soot and NO_x over $LaAgMnO_3$ catalyst. *Appl. Catal. A Gen.* **2019**, *588*, 117280. [CrossRef]
12. Wang, R.; Zhong, C.; Li, D.; Yu, X.; Zhao, Z.; Sojka, Z.; Kotarba, A.; Wei, Y.; Liu, J. Preparation of 3DOM $ZrTiO_4$ support, W_xCeMnO_δ/3DOM $ZrTiO_4$ catalysts, and their catalytic performance for the simultaneous removal of soot and NOx. *Front. Chem.* **2022**, *10*, 880884. [CrossRef]
13. Davies, C.; Thompson, K.; Cooper, A.; Golunski, S.; Taylor, S.H.; Bogarra Macias, M.; Doustdar, O.; Tsolakis, A. Simultaneous removal of NOx and soot particulate from diesel exhaust by in-situ catalytic generation and utilisation of N_2O. *Appl. Catal. B Environ.* **2018**, *239*, 10–15. [CrossRef]
14. Cooper, A.; Davies, T.E.; Morgan, D.J.; Golunski, S.; Taylor, S.H. Influence of the preparation method of Ag-K/CeO_2-ZrO_2-Al_2O_3 catalysts on their structure and activity for the simultaneous removal of soot and NOx. *Catalysts* **2020**, *10*, 294. [CrossRef]
15. Chen, L.; Li, J.; Ge, M. The poisoning effect of alkali metals doping over nano V_2O_5–WO_3/TiO_2 catalysts on selective catalytic reduction of NOx by NH_3. *Chem. Eng. J.* **2011**, *170*, 531–537. [CrossRef]
16. Rinkenburger, A.; Toriyama, T.; Yasuda, K.; Niessner, R. Catalytic Effect of Potassium Compounds in Soot Oxidation. *ChemCatChem* **2017**, *9*, 3513–3525. [CrossRef]
17. Ramdas, R.; Nowicka, E.; Jenkins, R.; Sellick, D.; Davies, C.; Golunski, S. Using real particulate matter to evaluate combustion catalysts for direct regeneration of diesel soot filters. *Appl. Catal. B Environ.* **2015**, *176–177*, 436–443. [CrossRef]
18. Jiang, Y.; Gao, X.; Zhang, Y.; Wu, W.; Luo, Z.; Cen, K. Effect of KCl on the Selective Catalytic Reduction of NO with NH_3 over Vanadia-Based Catalysts for Biomass Combustion. *Environ. Prog. Sustain. Energy* **2014**, *33*, 390–395. [CrossRef]
19. Twigg, M.V. An essay book review of 'Urea-SCR technology for deNOx after treatment of diesel exhausts'. *Johns. Matthey Technol. Rev.* **2015**, *59*, 221–232. [CrossRef]
20. Janoš, P.; Hladík, T.; Kormunda, M.; Ederer, J.; Šťastný, M. Thermal treatment of cerium oxide and its properties: Adsorption ability versus degradation efficiency. *Adv. Mater. Sci. Eng.* **2014**, *2014*, 706041. [CrossRef]
21. Davies, C.; Mayer, A.; Gabb, J.; Walls, J.M.; Degirmenci, V.; Thompson, P.B.J.; Cibin, G.; Golunski, S.; Kondrat, S.A. Operando potassium K-edge X-ray absorption spectroscopy: Investigating potassium catalysts during soot oxidation. *Phys. Chem. Chem. Phys.* **2020**, *22*, 18976–18988. [CrossRef]
22. Gill, L.J.; Blakeman, P.G.; Twigg, M.V.; Walker, A.P. The use of NOx adsorber catalysts on diesel engines. *Top. Catal.* **2004**, *28*, 157–164. [CrossRef]
23. Jayakumar, G.; Irudayaraj, A.; Raj, A.D.; Irudayaraj, A.A. Particle size effect on the properties of cerium oxide (CeO_2) nanoparticles synthesized by hydrothermal method. *Mech. Mater. Sci. Eng.* **2017**, *9*, 127–131.
24. Ghamsari, M.S.; Mahzar, Z.A.S.; Radiman, S.; Hamid, A.M.A.; Khalilabad, S.R. Facile route for preparation of highly crystalline γ-Al_2O_3 nanopowder. *Mater. Lett.* **2012**, *72*, 32–35. [CrossRef]
25. Halvarsson, M.; Langer, V.; Vuorinen, S. Determination of the thermal expansion of K-Al_2O_3 by high temperature XRD. *Surf. Coat. Technol.* **1995**, *76–77*, 358–362. [CrossRef]
26. Guha, P.; Juluri, R.R.; Bhukta, A.; Ghosh, A.; Maiti, S.; Bhattacharyya, A.; Srihari, V.; Satyam, P.V. In situ synchrotron X-ray diffraction study of coherently embedded silver nanostructure growth in silicon. *CrystEngComm* **2017**, *19*, 6811–6820. [CrossRef]
27. Cai, Y.; Wang, C.-B.; Wachs, I.E. Reaction induced spreading of metal oxides: In Situ Raman spectroscopic studies during oxidation reactions. *Stud. Surf. Sci. Catal.* **1997**, *110*, 255–264.
28. Fino, D.; Bensaid, S.; Piumetti, M.; Russo, N. A review on the catalytic combustion of soot in diesel particulate filters for automotive applications: From powder catalysts to structured reactors. *Appl. Catal. A Gen.* **2016**, *509*, 75–96. [CrossRef]

29. Foo, R.; Vazhnova, T.; Lukyanov, D.B.; Millington, P.; Collier, J.; Rajaram, R.; Golunski, S. Formation of reactive Lewis acid sites on Fe/WO_3-ZrO_2 catalysts for higher temperature SCR applications. *Appl. Catal. B Environ.* **2015**, *162*, 174–179. [CrossRef]
30. Jabłońska, M.; Palkovits, R. It is no laughing matter: Nitrous oxide formation in diesel engines and advances in its abatement over rhodium-based catalysts. *Catal. Sci. Technol.* **2016**, *6*, 7671–7687. [CrossRef]
31. Matsukata, M.; Fujikawa, T.; Kikuchi, E.; Morita, Y. Interaction between potassium carbonate and carbon substrate at subgasification temperatures. Migration of potassium into the carbon matrix. *Energy Fuels* **1988**, *2*, 750–756. [CrossRef]